

## Characterization and Functional Assessment of Mouse PPAR $\gamma$ 1 Promoter

Liana Lachinani<sup>1</sup>, Kamran Ghaedi<sup>1,2\*</sup>, Somayeh Tanhaei<sup>1</sup>, Ahmad Salamian<sup>1</sup>,  
Fereshteh Karamali<sup>1</sup>, Abbas Kiani-Esfahani<sup>1</sup>, Farzaneh Rabiee<sup>1</sup>, Parichehreh Yaghmaei<sup>5</sup>,  
Hossein Baharvand<sup>3,4</sup>, and Mohammad Hossein Nasr-Esfahani<sup>1\*</sup>

1. Department of Cell and Molecular Biology, Cell Science Research Center, Royan Institute for Animal Biotechnology, ACECR, Isfahan, Iran

2. Department of Biology, School of Sciences, University of Isfahan, Isfahan, Iran

3. Department of Developmental Biology, University of Science and Culture, ACECR, Tehran, Iran

4. Department of Stem Cells and Developmental Biology, Cell Science Research Center, Royan Institute for Stem Cell Biology and Technology, ACECR, Tehran, Iran

5. Department of Biology, Science and Research Branch, Islamic Azad University, Tehran, Iran

### Abstract

**Background:** Peroxisome Proliferator Activated Receptor gamma (PPAR $\gamma$ ), a member of nuclear receptor superfamily, comprises two isoforms in mouse. These two isoforms are encoded by different mRNAs, which are arisen by alternative promoter usage. There are two promoter regions upstream of PPAR $\gamma$  gene. A 3 kb fragment, containing several transcription factor binding sites, acts as PPAR $\gamma$ 1 promoter region. Thus, expression pattern of PPAR $\gamma$ 1 isoform is due to the potential transcription factors that could influence its promoter activity. PPAR $\gamma$ , Retinoid X Receptor (RXR) and Vitamin D Receptor (VDR), as nuclear receptors could influence PPAR $\gamma$  gene expression pattern during several differentiation processes. During neural differentiation, PPAR $\gamma$ 1 isoform expression reaches to maximal level at neural precursor cell formation.

**Methods:** A vast computational analysis was carried out to reveal the PPAR $\gamma$ 1 promoter region. The putative promoter region was then subcloned upstream of an EGFP reporter gene. Then the functionality of PPAR $\gamma$ 1 promoter was assessed in different cell lines.

**Results:** Results indicated that Rosiglitazone increased PPAR $\gamma$ 1 promoter regulated EGFP expression of neural precursor cells during Embryoid Body (EB) formation. Furthermore vitamin D reduced PPAR $\gamma$ 1 promoter regulated EGFP expression of neural precursor cells during EB formation through binding to its receptor.

**Conclusion:** This study suggests that there are potential response elements for PPAR/RXR and VDR/RXR heterodimers in PPAR $\gamma$ 1 isoform promoter. Also VDR/RXR heterodimers may decrease PPAR $\gamma$  expression through binding to its promoter.

*Avicenna J Med Biotech 2012; 4(4): 160-169*

**Keywords:** PPAR gamma, Mouse, Gene expression

\* **Corresponding authors:**  
Kamran Ghaedi, Ph.D. and  
Mohammad Hossein Nasr-  
Esfahani, Ph.D., Department  
of Cell and Molecular Biolo-  
gy, Cell Science Research  
Center, Royan Institute for  
Animal Biotechnology,  
ACECR, Isfahan, Iran  
**Tel:** +98 311 2612900  
**Fax:** +98 311 2605525  
**E-mail:** kamranghaedi  
@royaninstitute.org; mh.nasr-  
esfahani@royaninstitute.org  
**Received:** 23 Apr 2012  
**Accepted:** 3 Jul 2012

### Introduction

Peroxisome Proliferator Activated Receptors (PPARs) are ligand-activated transcription factors belong to nuclear hormone recep-

tor superfamily. There are three different isoforms of PPARs: PPAR $\alpha$ , PPAR $\beta/\delta$  and PPAR $\gamma$ , encoded by separate genes on differ-

ent chromosomes. These isoforms exert different functions in the cell and show differential tissue distribution pattern. The main roles of PPARs include cell differentiation, development, and metabolism of macromolecules. The functions of PPARs are mediated through their activation by specific ligands including naturally occurring fatty acids or fatty acid derivatives. To complete this scenario, heterodimerization of PPARs with the RXR is required for binding to specific response elements termed: Peroxisome Proliferator Response Element (PPRE) at promoter region of target genes. PPRE consists of hexameric Direct Repeat (DR) pattern (AGGTCA) with a single nucleotide between each hexameric motif. PPAR/retinoid X receptor (RXR) heterodimers bind to these response elements through the PPAR DNA binding domain, which is a highly conserved domain similar to various transcription factors<sup>(1,2)</sup>.

Among PPARs, PPAR $\gamma$  is mainly involved in adipose tissue differentiation and maintenance of adipocyte specific functions. Moreover, it also plays a role in homeostasis of glucose, cholesterol, and insulin sensitivity. Recently, functions of PPAR $\gamma$  in reduction of inflammation, and cell cycle withdrawal have been elucidated<sup>(3,4)</sup>. Besides the mentioned roles, recently we have demonstrated a stage dependent role of PPAR $\gamma$  modulation during neural differentiation of mouse Embryonic Stem Cells (mESC) by retinoic acid treatment<sup>(5)</sup>. Mouse PPAR $\gamma$  consists of two isoforms, PPAR $\gamma$ 1 and PPAR $\gamma$ 2. Longer isoform (PPAR $\gamma$ 2) contains an extra 30 amino acid residues at the amino terminus<sup>(6)</sup>. Both isoforms differ in their expression patterns and tissue distribution. PPAR $\gamma$ 1 is mainly distributed in heart, muscle, liver and colon, while, PPAR $\gamma$ 2 is highly expressed in the adipose tissue<sup>(7)</sup>.

Productions of these isoforms are under regulation of alternative promoters and different splicing of PPAR $\gamma$  gene. Mouse PPAR $\gamma$  gene comprises 105 kb located at E3-F1 region of chromosome 6. mRNAs of PPAR $\gamma$ 1 and PPAR $\gamma$ 2 consisting of eight and seven

exons, respectively. Six exons are shared in the structure of both PPAR $\gamma$  isoforms. There are extra exons encoding 5'-untranslated regions that are present in the structure of both isoforms. Promoter regions of PPAR $\gamma$  isoforms are distanced 40 kb far from each other, and therefore, they are responsible for different specific expression patterns in several organisms and tissues<sup>(6)</sup>. An intense study of these promoter regions with evaluation of their potential response elements are required to clarify the differential mechanisms of PPAR $\gamma$  isoforms expression. In the present study, we have constructed essential elements of PPAR $\gamma$ 1 promoter upstream of EGFP cDNA as a reporter gene to provide a suitable system for evaluation of this region and containing response elements.

## Materials and Methods

### Bioinformatics studies

To predict putative promoter regions of mouse PPAR $\gamma$ 1 isoform, approximately 200 kb upstream region of PPAR $\gamma$  gene (NC\_000072.5) was selected for analysis by Genomatix software (<http://www.genomatix.de>). Furthermore, presence of Transcription Factor Binding Sites (TFBS) in predicted PPAR $\gamma$ 1 promoter region was analyzed by several online softwares including Genomatix, TESS (<http://www.cbil.upenn.edu>), Gene Builder (<http://www.itb.cnr.it/sun/webgene>) and TFS EARCH (<http://www.cbrc.jp/research/db/TFSEARCH.html>). The sequence data are shown in figure 1 and predicted TFBS are demonstrated in table 1.

### PCR amplification of PPAR $\gamma$ 1 promoter region

DNA was derived from Mouse Embryonic Fibroblast (MEF) cells which were obtained from the Department of Stem cells and Developmental biology (Royan Institute for Stem Cell Biology and Technology) and used as a template in PCR. Specific primers for amplification of predicted PPAR $\gamma$ 1 promoter region, -2954 to +178 bp relative to Open Reading Frame (ORF) of PPAR $\gamma$ 1, were designed using Oligo6.71 software, introducing

## Mouse PPAR $\gamma$ Promoter Characterization

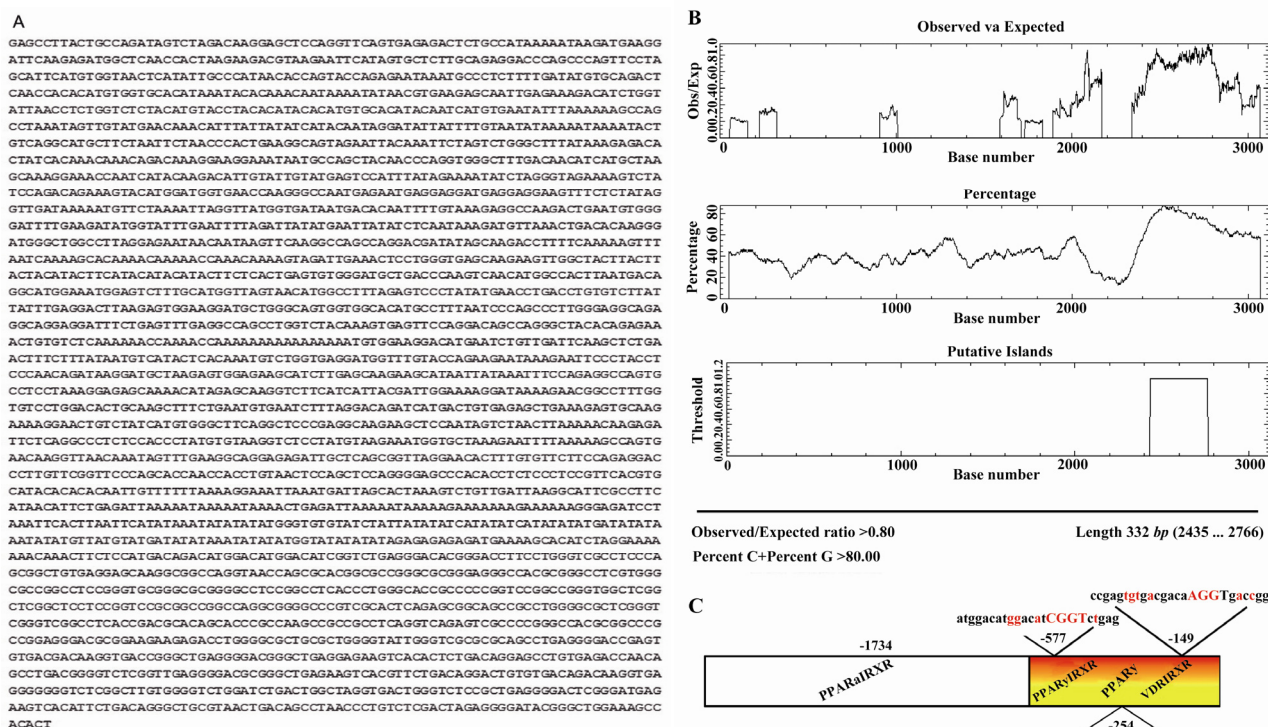


Figure 1. Sequence of mouse PPAR $\gamma$  putative core-promoter. A) PPAR $\gamma$ 1 promoter region sequence. B) CpG plot of PPAR $\gamma$ 1 core-promoter region (EMBL-EBI: <http://www.ebi.ac.uk/Tools/emboss/cpgplot/index.html>). C) Diagram of GC rich region of PPAR $\gamma$ 1 promoter region and predicted response elements on it

Table 1. Predicted transcription factor binding sites for mouse PPAR $\gamma$ 1 promoter

Response element	Sequence (5' - 3')	Position	Score	
			TESS* (Lq**)	Genomatix (Matrix similarity***)
PPAR <sup>1</sup>	CCTCAGGTCAGAGTCGCCCCGGG	2701	1	0.675
PPAR-RXR <sup>2</sup>	ATGGACATGGACATCGGTCTGAG	2379	--	0.785
PPAR-RXR	TGACCTNTGTCCT	1200	0.917	--
VDR-RXR <sup>3</sup>	CCGAGTGTGACGACAAGGTGACCGG	2806	--	0.753
AP-2 <sup>4</sup>	GCCGCCTGGGGCGCT	2640	1	0.935
AP-2	GCAGCCTGAGGGGAC	2792	1	0.971

\*TESS: Transcription element search software on the WWW.

\*\*Lq: The ratio of  $L_a / L_M$ , where  $L_M$  is the maximum  $L_a$  possible for the site model. The best score is 1.0. Thus  $L_a / L_M$  is the ratio of log-likelihood score to the length of the site. The best score for  $L_a / L_M$  is 2.0. For further information please see the following site: <http://www.cbil.upenn.edu/cgi-bin/tess/tess?RQ=MRZ-leg&job=W0502026399&is=1&nr=50&att=beg&fr=0&mask=-1>.

\*\*\*Matrix similarity: The matrix similarity is calculated as described in

[http://www.genomatix.de/online\\_help/help/scores.html?s=b66803c222e3ce9257cd2e748b244230#msim](http://www.genomatix.de/online_help/help/scores.html?s=b66803c222e3ce9257cd2e748b244230#msim).

A perfect match to the matrix gets a score of 1.00 (each sequence position corresponds to the highest conserved nucleotide at that position in the matrix), a "good" match to the matrix usually has a similarity of >0.80.

<sup>1</sup> Peroxisome proliferator-activated receptor

<sup>2</sup> PPAR heterodimer with retinoid X receptor

<sup>3</sup> Vitamin D receptor heterodimer with retinoid X receptor

<sup>4</sup> Activator protein 2

*VspI* and *NheI* recognition sites at flanking regions of forward and reverse primers, respectively (Table 2), and ordered through Metabion Company (Germany). PCR reactions were performed using *ExTaq* poly-

merase (TaKaRa) according to the following protocol: First denaturation was achieved at 94 °C for 5 min. Amplification reactions were carried out in 35 repetitive cycles during three steps, 45 s at 94 °C, 45 s at 60 °C, and 1 min at

Table 2. List of primers used in this study

Gene	Primer sequence (5'-3')	Annealing temp (°C)	Accession no.	Product length
<i>PPAR<math>\gamma</math>1</i>	F1: <u>GATTAAT</u> AGCCTTACTGCCAGATAGTCTA(-2954) <i>VspI</i>	61	NC_000072.5	1190 bp
	R1: TAAAGGCCATGTTACTAACCA (-1764)			
	F2: GCTGGCCTTAGGAGAATAACAATA (-2039)	65		1040 bp
	R2: TGTTCTAACCGCTGAGCA (-999)			
	F3: AGCTGAAAGAGTGCAAGAAAAGGAACTGTCTATC (-1224)	60		671 bp
	R3: CTCAGACCGATGTCCATGTCCATGTC (-553)			
	F4: GATTAGCACTAAAGTCTGTTGATTAAGGCATTTCG (-854)	58.3		1032 bp
	R4: GTT <u>GCTAGC</u> TTTCCAGCCCGTATCCCCTCTAG (+178) <i>NheI</i>			
<i>EGFP</i>	F: CAAGCAGAAGAACGGCATCAAG	63		145 bp
	R: GGTGCTCAGGTAGTGGTTGTC			
<i>GAPDH</i>	F: TGCCGCCTGGAGAAACC	60	NM_008084.2	121 bp
	R: TGAAGTCGCAGGAGACAACC			

F and R, are referred as forward and reverse primers, respectively. Restriction sites are underlined

72 °C for denaturation, annealing and extension respectively. Finally, PCR reactions terminated at 72 °C for 10 min.

Total fragment of PPAR $\gamma$ 1 promoter was amplified by Splicing and Overlapping Extension PCR (SOE-PCR) method of four fragments: F1R1 (1190 bp), F2R2 (1040 bp), F3R3 (671 bp) and F4R4 (1032 bp). At first F1R1, F2R2 and F3R3 fragments were amplified and sub-cloned into pTZ57R/T to make one fragment. These fragments demonstrated approximately 100 bp overlapping. The fourth fragment, F4R4, also was amplified and separately sub-cloned into pTZ57R/T. Two constructs were double-digested by *XcmI* and *BamHI* and re-ligated at *XcmI* site to produce total PPAR $\gamma$ 1 promoter fragment, F1R4. Finally, total length fragment with *VspI-NheI* overhangs from pTZ57R/T was sub-cloned into pDB2 target vector (Figure 2).

Amplification of F4R4 fragment (a fragment of about 1 kb) containing a highly GC rich region, was achieved by implementing AMS (Ammonium Sulfate) in reaction to buffer supplemented with 3% DMSO, 0.25 M

betaine, 7-deaza dGTP (with 3:1 ratio to normal dGTP).

#### Plasmid constructions

Amplified fragment of DNA containing PPAR $\gamma$ 1 promoter region (3.1 kb) was purified by ethanol precipitation method after gel extraction and inserted into pTZ57R/T vector (Fermentas) using DNA ligation kit (TaKa Ra). Upon blue-white screening of transformed bacterial colonies [DH5 $\alpha$  strain of *Escherichia coli* (*E.coli*), Fermentas], screening was performed to select those bacterial colonies which contained recombinant plasmid. Thus, positive white colonies were assessed by insert check PCR experiment using T7 and specific promoter primers (Table 2).

Plasmid extraction from positive colonies was carried out using plasmid mini prep kit (Qiagen). Recombinant vectors were sent for sequencing of the insert DNA (Faza Pajouh, Iran). At the next step, PPAR $\gamma$  promoter region was extracted from pTZ57R/T recombinant vectors by *VspI* and *NheI* double-digestion and inserted into the same sites in pDB2 vector (kindly provided by Prof. M

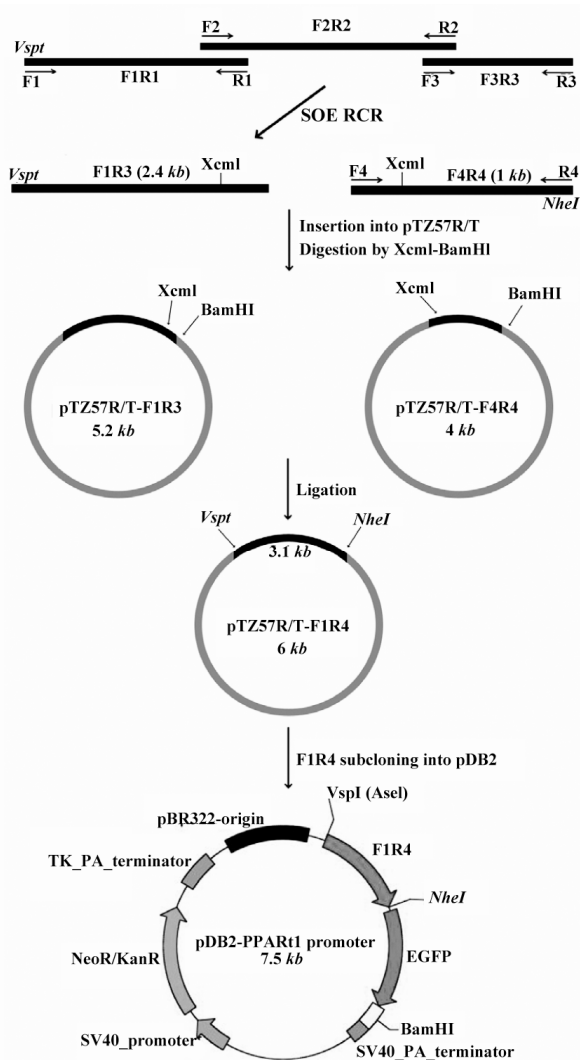


Figure 2. Schematic representation of PCR amplification of PPAR $\gamma$ 1 promoter region by SOE-PCR and subcloning into pDB2 reporter vector

Calus, University of Stanford) in place of CMV promoter region and termed pDB2/PPAR $\gamma$ 1.

To construct a promoter free vector, CMV promoter was pulled out from the backbone of pDB2 vector by a *VspI-NheI* double digestion. *VspI-NheI* double-digested plasmid backbone was treated by Klenow fragment (Fermentas) at 37 °C for 30 min to blunt its sticky ends. Re-ligation was performed to form a circular pDB2 vector without promoter. Finally, recombinant vectors were amplified by transformation in to the DH5 $\alpha$  strain of *E.coli* (Fermentas). Bacterial colonies were checked by PCR insert check analysis.

### Cell culture and transfection

CHO-K1 cells were cultured in DMEM/Ham's F-12 (Sigma, D8900) medium supplied with 100 U/ml penicillin (Gibco, 15070) under a humidified atmosphere at 5% CO $_2$ . CHO cells were plated in density of 1.3x10 $^4$  cells/cm $^2$ . When cells reached to 50-80% of confluency, transfection was carried out by pDB2/PPAR $\gamma$ 1 promoter, pDB2 and promoter free pDB2 vectors by lipofectamine 2000 (Invitrogen) according to the manufacturer's instruction. After 48 hr of transfection, the cells were fixed by 4% para formaldehyde/PBS buffer for 30 min. Meanwhile, nuclei were stained with 4,6-diamidino-2-2- phenylindole (DAPI) for 3 min at room temperature. Green fluorescence of cells was assessed with a fluorescent microscope (Olympus, Japan) and images were taken with an Olympus D70 camera (Olympus, Japan).

### Generating stably transformed mouse embryonic stem cells and embryoid body formation and treatments

Mouse embryonic stem cells (mESCs, Royan B1 cells)<sup>(8)</sup> were cultured in KDMEM (Gibco) with 15% ES-FCS (Gibco), 0.1 mM  $\beta$ -mercaptoethanol (Sigma-Aldrich), 2 mM glutamine (Gibco), 0.1 mM non-essential amino acids (Sigma-Aldrich) and 1000 U/ml Leukemia Inhibitory Factor (LIF, Chemicon). mESCs were plated in density of 7.8x10 $^4$  cells/cm $^2$  in gelatin coated 12-well Tissue Culture Plates (TPP). Transfection was carried out using pDB2/PPAR $\gamma$ 1 promoter recombinant vector and lipofectamine 2000 (Invitrogen) according to the manufacturer's instruction. After 48 hr of transfection, cells were plated on MTK-Neo feeder cells in the presence of 800  $\mu$ g/ml of G418 (Sigma). Finally, 24 days later resistant colonies were grown and analyzed by genomic PCR. Stably transformed mESCs were cultured in hanging drops to form Embryoid Bodies (EBs) for two days as previously reported<sup>(9)</sup>. EBs were collected and moved to suspension culture in presence of reduced amounts of serum (10%), 1  $\mu$ M of retinoic acid (Sigma-Aldrich) and G418 (400  $\mu$ g/ml) for four days.

During the aforementioned 4 days treatment, cells were simultaneously treated with one of the following components: specific PPAR $\gamma$ 1 agonists, Rosiglitazone (Cayman Chemical; 5  $\mu$ M) or selective specific antagonist, GW9662 (Sigma; 10  $\mu$ M) or Calcitriol (Sigma; 10<sup>-8</sup> M). Furthermore, cells were treated by DMSO (10  $\mu$ l) or ethanol (5  $\mu$ l) as vehicles for PPAR $\gamma$  agonist, antagonist and Calcitriol (Vitamin D), respectively. On the sixth day, the EBs were collected for real time PCR analysis as previously described<sup>(5)</sup>.

#### **RNA extraction and cDNA synthesis**

Total RNAs from transiently transfected CHO-K1 cells and EBs were extracted using RNeasy Mini Kit (Qiagen). Extracted RNAs were treated by *DNase* I (Fermentas) to remove possible DNA contamination. About 1  $\mu$ g of total RNA of each sample was used for synthesis of the first strand cDNA using random hexamer primers supplied by Revert Aid First Strand cDNA Synthesis Kit (Fermentas).

#### **Real time PCR**

Real time PCR reactions were carried out using 5  $\mu$ l SYBR GreenPCR Master Mix (Takara) and 0.25 *pM* of specific primers (Table 2), 25 *ng* of cDNA in total volume of 10  $\mu$ l. All reactions were held in triplicates and normalized by GAPDH. All data's were analyzed by  $\Delta\Delta$ Ct method.

#### **Flow cytometry**

To quantify the fluorescence intensity of EGFP, transiently transfected CHO-K1 cells were detached by Trypsin/EDTA (Gibco), 48 *hr* post-transfection and analyzed by Becton Dickinson FACS Caliber flow cytometer (USA) as follows: for each sample, 10<sup>4</sup> events were recorded in the forward light scatter/side light scatter (FSC/SSC) dot plot. Then a gate was used to select single cells from aggregated and debris.

Green fluorescence of EGFP was detected in the fluorescence detector 1 (FL-1) with a 530/30 *nm* band pass filter. Data obtained from flow cytometer instrument were analyzed by using Cell-Quest Pro and WinMDI

2.9 software. To reduce the transfection efficiency effect, this experiment was done three times independently and the average of fluorescence intensity was calculated and considered for analysis.

#### **Statistical analyses**

Data were expressed as means $\pm$ SEM obtained from three independent replicates of observations. Differences between the expression patterns of the samples were determined using student's t-test and were judged to be significant at *p*<0.01 and 0.05.

## **Results**

### **Bioinformatics studies of PPAR $\gamma$ 1 promoter region and amplification of target region**

Based on bioinformatics studies, six potential promoter upstream regions of PPAR $\gamma$  gene were predicted. According to transcription initiation site only one of these potential regions was able to be used for encoding PPAR $\gamma$ 1 mRNA. This region was similar to the previously determined PPAR $\gamma$ 1 promoter region with little differences in several nucleotides. Thus, considering the previous studies<sup>(6)</sup>, 3.1 *kb* DNA fragment was selected and analyzed for presence of possible TFBS (Figure 1A). Data predicted presence of several putative TATA boxes (Table 1). This fragment was characterized as a highly GC rich fragment (about 1 *kb*) with >80% CG content and 332 *bp* of CpG island (Figure 1B). According to bioinformatics results from Genomatix, TESS, GeneBuilder and TFSEARCH softwares, different TFBSs were predicted at this promoter region (Table 2). Among the predicted sequences, there were response elements for VDR-RXR and PPAR-RXR heterodimers and PPAR $\gamma$  homodimer binding sites (Figure 1C).

### **PPAR $\gamma$ 1 promoter region subcloning and promoter activity confirmation**

PPAR $\gamma$ 1 promoter regions were successfully amplified as F1R1 (1190 *bp*), F2R2 (1040 *bp*), F3R3 (671 *bp*) and F4R4 (1032 *bp*) (Figure 3). As described in material and methods, F1R1, F2R2 and F3R3 fragments were ampli-

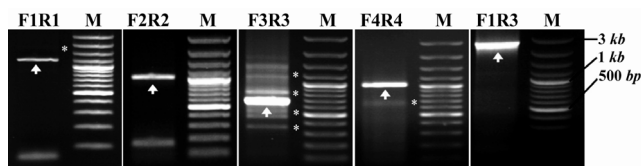


Figure 3. PCR steps for constructing different PPAR $\gamma$ 1 promoter region. PCR-product bands: the molecular size marker [100 bp; Fermentas] (M) and four fragments of PPAR $\gamma$ 1 promoter region; F1R1 (1190 bp), F2R2 (1040 bp), F3R3 (671 bp) and F4R4 (1032 bp) are indicated by arrow heads. Stars indicate nonspecific bands

fied and sub-cloned into pTZ57R/T to make one fragment. The fourth fragment, F4R4, also was amplified and separately sub-cloned into pTZ57R/T.

At the next step, whole of the PPAR $\gamma$ 1 promoter region was successfully amplified and cloned into pDB2 target vector. CMV promoter of pDB2 vector was removed by *VspI* and *NheI* digestion and PPAR $\gamma$ 1 promoter region was replaced at corresponding sites. Thus, in pDB2/PPAR $\gamma$ 1 promoter recombinant vector, expression of EGFP reporter gene was under regulation of PPAR $\gamma$ 1 promoter region (Figure 2). To confirm PPAR $\gamma$ 1 promoter activity, pDB2-PPAR $\gamma$ 1 promoter recombinant vector was transfected into CHO-K1 cells. After 48 hr of transfection, green fluorescence was observed in cells and confirmed promoter activity and functionality of recombinant vector (Figures 4E and 4H). Simultaneously, original vector of pDB2, containing CMV promoter and promoter-lacking pDB2 vector were transfected into CHO cells. Cells transfected by original pDB2 vector expressed EGFP at high levels (Figures 4A, 4D and 4G) when compared with untransfected cells (Figures 4C, 4F and 4I). Whereas, promoter-lacking pDB2 vector transfection had no EGFP expression result (data not shown).

To evaluate and compare EGFP expression levels under control of PPAR $\gamma$ 1 promoter, flow cytometric analysis was performed. Data showed a reduced EGFP expression pattern under control of PPAR $\gamma$ 1 promoter relative to viral CMV promoter. These data implicated that relative activity of PPAR $\gamma$ 1 promoter is about 0.2 fold of CMV promoter (Figure 4J).

Furthermore, to evaluate the functionality of PPAR $\gamma$ 1 promoter in another cell line, stably transformed mESCs with the recombinant vector (pDB2-PPAR $\gamma$ 1 promoter) was implemented for analysis of the EGFP expression level. Real time PCR analysis revealed significant difference in EGFP expression level in stably transformed mESCs compared to the untransfected mESCs (Figure 4K).

As several response elements for VDR-RXR and PPAR-RXR heterodimers and PPAR $\gamma$  homodimer binding sites were identified in putative PPAR $\gamma$ 1 promoter region, the effects of PPAR $\gamma$  agonist (Rosiglitazone), PPAR $\gamma$  antagonist (GW9662) and vitamin D (Calcitriol) on promoter activity of PPAR $\gamma$ 1 promoter were assessed using real time PCR analyses for EGFP expression. We have already shown that 5  $\mu$ M of Rosiglitazone and 10  $\mu$ M of GW 9662 caused activation and inactivation of PPAR $\gamma$ , respectively as nuclear localization of PPAR $\gamma$  increased upon activation and decreased during inactivation<sup>(5,10)</sup>. Our results indicated that Rosiglitazone increased PPAR $\gamma$ 1 promoter regulated EGFP expression of neural precursor cells during EB formation (Figure 4L). Thus, it seems that active heterodimers of PPAR $\gamma$ /RXR interact with PPAR $\gamma$ 1 promoter region and this region contains potential response elements for PPAR $\gamma$ /RXR heterodimers. On other hand, GW9662, potent antagonist of PPAR $\gamma$ , reduced EGFP expression in these cells (Figure 4L).

Due to the recently published function of vitamin D in nervous system, the effect of vitamin D was examined on EGFP expression in stably transformed mESCs that underwent neural precursor cell formation. Data revealed vitamin D reduced PPAR $\gamma$ 1 promoter regulated EGFP expression of neural precursor cells during EB formation through binding to its receptor (Figure 4L).

### Discussion

PPARs are members of the nuclear-receptor superfamily of proteins and act as nuclear transcription factors where they form

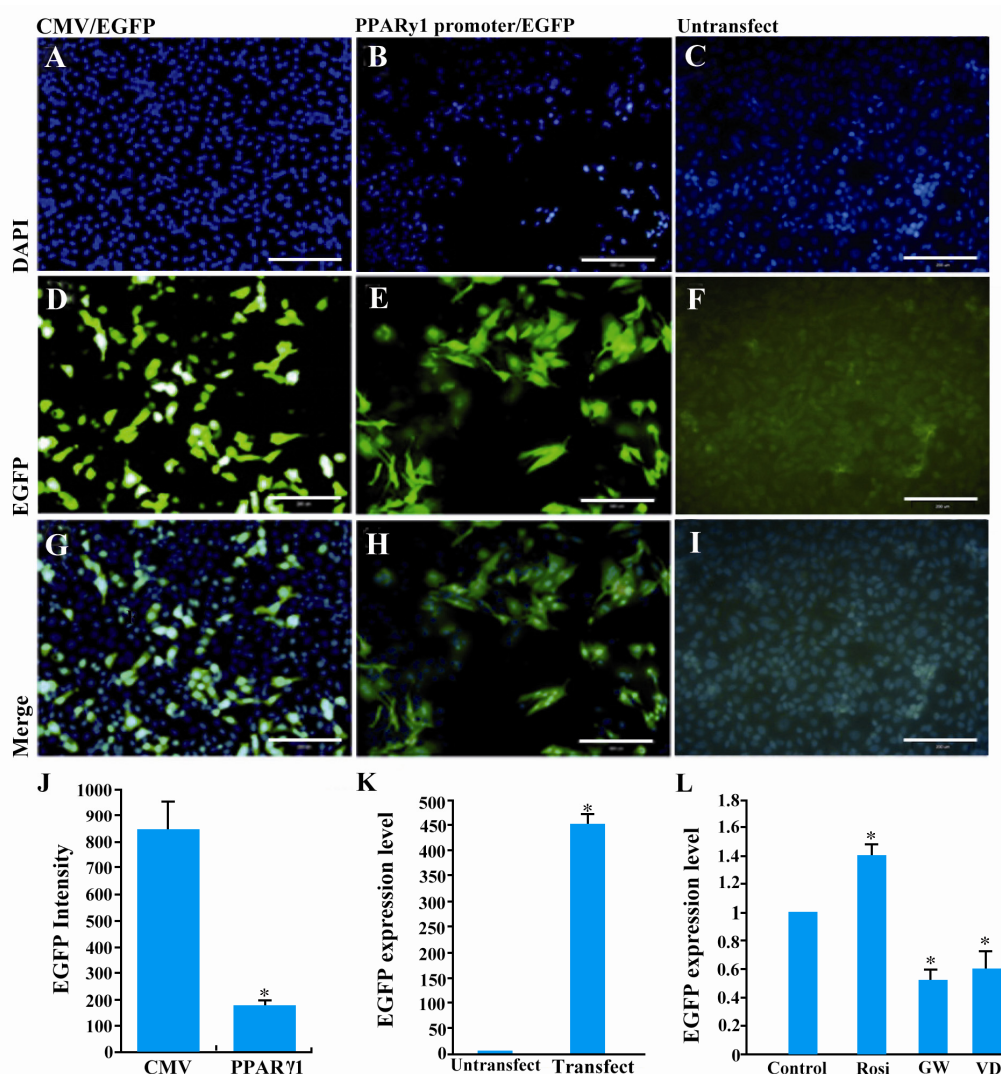


Figure 4. Assessment of the functional activity of PPAR $\gamma$ 1 promoter. Transiently transfected CHO cells by pDB2 vector (A, D, G) and pDB2-PPAR $\gamma$ 1 promoter vector (B, E, H) and untransfected cells (C, F, I). As shown in this figure, the cloned fragment was *bona fide* part of PPAR $\gamma$ 1 promoter region with a weaker activity than CMV promoter. Nuclei counterstaining with DAPI (upper panel), EGFP fluorescence (middle panel), merged figures (lower panel) are shown. J) Comparison of PPAR $\gamma$ 1 promoter activity with CMV promoter using flow cytometry as indicated PPAR $\gamma$ 1 promoter is a weaker promoter than CMV. K) *EGFP* expression level in stably transformed mESCs by pDB2-PPAR $\gamma$ 1 promoter vector compared with untransfected cells showing functional activity for PPAR $\gamma$ 1 promoter. L) Treatment of stably transfected mESCs by Rosiglitazone (Rosi: 5  $\mu$ M) or GW9662 (GW: 10  $\mu$ M) or Calcitriol (VD:10<sup>-8</sup> M) as described in materials and methods. As predicted at this promoter region (Table 2), there were response elements for VDR-RXR and PPAR-RXR heterodimers and PPAR $\gamma$  homodimer binding sites (Figure 1C). *EGFP* expression levels in these cells were compared with untreated stably transformed mESCs by pDB2-PPAR $\gamma$ 1 promoter by real time PCR. In this study, treatment of stably transfected mESCs by Rosiglitazone and GW9662, increased and decreased PPAR $\gamma$  promoter activity 1.5 and 0.5 fold, respectively. Moreover, vitamin D reduced PPAR $\gamma$ 1 promoter regulated *EGFP* expression in neural precursor cells (approximately 40%). Scale bar is 200  $\mu$ m

a heterodimer with the Retinoid X Receptor (RXR). The PPAR-RXR heterodimer binds to PPAR Response Elements (PPRE) in the promoter of PPAR-responsive genes<sup>(1,3,11)</sup>. Among various PPARs, PPAR $\gamma$  consists of two different isoforms (PPAR $\gamma$ 1 and PPAR $\gamma$ 2) because of alternative processing of PPAR $\gamma$  mRNA.

In this manuscript, cloning of PPAR $\gamma$ 1 promoter is reported and its subfunctionality through construction of a vector regulating *EGFP* expression is approved. However, the strength of PPAR $\gamma$ 1 was estimated to be 20% of the CMV promoter. Bioinformatics studies revealed presence of different transcription factor-response elements at promoter region



of mouse PPAR $\gamma$  gene. The functionality of response elements for PPAR/RXR and VDR/RXR at promoter region of mouse PPAR $\gamma$ 1 isoform was pinpointed. PPAR $\gamma$  and vitamin D activated receptor exert their activity through binding to specific DNA sequences at promoter region of target genes. Their binding to specific response elements requires heterodimerization with RXR<sup>(3,12)</sup>.

PPAR $\gamma$  is a transcription factor mainly expressed in adipose tissues. Our recent studies suggest that PPAR $\gamma$  also maintains a role in neural differentiation. During neural differentiation of mouse embryonic stem cells, expression of PPAR $\gamma$ 1 isoform is raised and reaches maximal level during neural precursor cell formation<sup>(5)</sup>. Treatment of mESC by retinoic acid during this procedure causes activation of RXR. In this stage Rosiglitazone, a synthetic PPAR $\gamma$  agonist, activates PPAR $\gamma$  and induces PPAR/RXR heterodimer formation. Subsequently, activated PPAR/RXR heterodimers could bind to PPREs in promoter regions of target genes.

Based on bioinformatics studies, there are predicted response elements of PPAR $\gamma$ /RXR and PPAR $\gamma$  at PPAR $\gamma$ 1 promoter region, respectively at -577 and -254 bp of PPAR $\gamma$ 1 ORF. In this study, treatment of stably transfected mESCs by GW9662, a PPAR $\gamma$  antagonist decreased PPAR $\gamma$  promoter activity to 0.5 fold of untreated cells. In addition, Rosiglitazone treatment caused an increase in PPAR $\gamma$  promoter activity. This data suggest that PPAR $\gamma$ /RXR heterodimers could regulate PPAR $\gamma$  expression by binding to respective response element at PPAR $\gamma$  promoter.

Vitamin D, as a nuclear hormone and its nuclear receptor (Vitamin D receptor) regulate transcription of several genes in neurons and neuronal precursor cells<sup>(13,14)</sup>. This nuclear receptor associates with vitamin D and forms heterodimers with RXR and exerts its activity through binding to vitamin D response elements of target genes. In adipocyte, vitamin D and VDR inhibit both PPAR $\gamma$  activity and adipogenesis<sup>(15)</sup>.

## Conclusion

Based on bioinformatics studies on PPAR $\gamma$ 1 promoter region, a potential VDR/RXR heterodimer response element was predicted at -149 bp of PPAR $\gamma$ 1 ORF. PPAR $\gamma$ 1 promoter activity in stably transfected mESCs after treatment by vitamin D was decreased to 0.7 fold of untreated cells at day 6 of EBs, when both PPAR $\gamma$  and RXR were transcriptionally active. We hypothesized that VDR/RXR heterodimers may decrease PPAR $\gamma$  expression through binding to its promoter. Clearly, more work is needed to develop a comprehensive understanding of the cellular and molecular mechanisms in regulating PPAR $\gamma$  expression by vitamin D.

## Acknowledgement

This study was supported by a grant from Royan Institute awarded to Kamran Ghaedi.

## References

1. Michalik L, Auwerx J, Berger JP, Chatterjee VK, Glass CK, Gonzalez FJ, et al. International Union of Pharmacology. LXI. Peroxisome proliferator-activated receptors. *Pharmacol Rev* 2006;58(4): 726-741.
2. Clarke SD, Thuillier P, Baillie RA, Sha X. Peroxisome proliferator-activated receptors: a family of lipid-activated transcription factors. *Am J Clin Nutr* 1999;70(4):566-571.
3. Berger J, Moller DE. The mechanisms of action of PPARs. *Annu Rev Med* 2002;53:409-435.
4. Fajas L, Debril MB, Auwerx J. Peroxisome proliferator-activated receptor-gamma: from adipogenesis to carcinogenesis. *J Mol Endocrinol* 2001;27(1):1-9.
5. Ghoochani A, Shabani K, Peymani M, Ghaedi K, Karamali F, Karbalaei K, et al. The influence of peroxisome proliferator-activated receptor  $\gamma$ 1 during differentiation of mouse embryonic stem cells to neural cells. *Differentiation* 2012;83(1):60-67.
6. Zhu Y, Qi C, Korenberg JR, Chen X, Noya D, Rao MS, et al. Structural organization of mouse peroxisome proliferator activated receptor  $\gamma$  (mPPAR $\gamma$ ) gene: Alternative promoter use and different splicing yield two mPPAR $\gamma$  isoforms. *Proc Natl Acad Sci USA* 1995;92(17):7921-7925.
7. Fajas L, Auboeuf D, Raspe E, Schoonjans K, Lefebvre A, Saladin R, et al. The organization, promot-

- er analysis, and expression of the human PPAR $\gamma$  gene. *J Biol Chem* 1997;272(30):18779-18789.
8. Baharvand H, Matthaie KI. Culture condition difference for establishment of new embryonic stem cell lines from the C57BL/6 and BALB/c mouse strains. *In Vitro Cell Dev Biol Anim* 2004;40(3-4):76-81.
  9. Ostadsharif M, Ghaedi K, Nasr-Esfahani MH, Mojibafan M, Tanhaie S, Karbalaie K, et al. The expression of peroxisomal protein transcripts increased by retinoic acid during neuronal differentiation. *Differentiation* 2011;81(2):127-132.
  10. Kapadia R, Yi JH, Vemuganti R. Mechanisms of anti-inflammatory and neuroprotective actions of PPAR-gamma agonists. *Front Biosci* 2008;13:1813-1826.
  11. Feige JN, Gelman L, Michalik L, Desvergne B, outputs: Peroxisome proliferator-activated receptors are nuclear receptors at the crossroads of key cellular functions. *Prog Lipid Res* 2006;45(2):120-159.
  12. Sertznig P, Seifert M, Tilgen W, Reichrath J. Activation of vitamin D receptor (VDR)- and peroxisome proliferator-activated receptor (PPAR)-signaling pathways through 1,25(OH) $_2$ D $_3$  in melanoma cell lines and other skin-derived cell lines. *Dermatoendocrinol* 2009;1(4):232-238.
  13. Levenson CW, Figueiroa SM. Gestational vitamin D deficiency: long-term effects on the brain. *Nutr Rev* 2008;66(12):726-729.
  14. Garcion E, Wion-Barbot N, Montero-Menei CN, Berger F, Wion D. New clues about vitamin D functions in the nervous system. *Trends Endocrinol Metab* 2002;13(3):100-105.
  15. Wood RJ. Vitamin D and adipogenesis: new molecular insights. *Nutr Rev* 2008;66(1):40-46.